Interlayer transverse magnetoresistance in the presence of an anisotropic pseudogap

M. F. Smith* and Ross H. McKenzie
Department of Physics, University of Queensland, Brisbane, Queensland 4072, Australia
(Received 9 July 2009; revised manuscript received 29 September 2009; published 23 December 2009)

The interlayer magnetoresistance of a quasi-two-dimensional layered metal with a *d*-wave pseudogap is calculated semiclassically. An expression for the interlayer resistivity as a function of the strength and direction of the magnetic field, the magnitude of the pseudogap, temperature, and scattering rate is obtained. We find that the pseudogap, by introducing low-energy nodal quasiparticle contours, smooths the dependence on field direction in a manner characteristic of its anisotropy. We thus propose that interlayer resistance measurements under a strong field of variable orientation can be used to fully characterize an anisotropic pseudogap. The general result is applied to the case of a magnetic field parallel to the conducting layers using a model band structure appropriate for overdoped Tℓ2201.

DOI: 10.1103/PhysRevB.80.214528 PACS number(s): 74.25.Fy, 74.72.−h, 72.15.Gd

I. INTRODUCTION

High-temperature superconducting cuprates, organic charge-transfer salts, some heavy fermion materials, and a host of other intriguing electronic systems, are layered metals in which electrons are approximately confined to a given atomic layer. Much of the interesting behavior of these materials arises because of strong electronic correlations within a single layer. Surprisingly, it turns out that one of the most effective means of accessing in-layer properties, particularly those properties that are highly anisotropic within a layer, is to measure *interlayer* electronic-transport coefficients in a strong magnetic field.[1–11]

The interlayer electrical resistivity ρ_{zz} depends on the direction of the magnetic field in a manner that is highly sensitive to the anisotropy of the quasi-two-dimensional (quasi-2D) band structure. High-resolution maps of the Fermi surface and other band-structure properties have already been obtained by fitting ρ_{zz} data to calculations based on semiclassical magnetotransport theory. This technique has been applied to a wide variety of layered materials including overdoped cuprates,[1–4] ruthenates,[5,6] and organic charge-transfer salts.[7,8] The ρ_{zz} data also contains information about in-plane scattering and can be used to study the directional dependence of elastic- and inelastic-scattering rates.[12–18] Notably, it has been used to reveal a *T*-linear, anisotropic scattering contribution in overdoped cuprate superconductors that appears to be tied to superconductivity itself.[2,19,20] It is important to press further, to ask what other anisotropic properties of the metallic layers can be detected and characterized via interlayer transport in high magnetic fields.

In this paper we ask what field-angle-dependent interplane transport data can tell us about an anisotropic pseudogap $\Delta_{\mathbf{k}}$ in quasi-2D metals. Since an anisotropic gap in the density of states will affect the field-direction dependence of ρ_{zz}, we expect that interlayer magnetoresistance can be used to map out $\Delta_{\mathbf{k}}$ as well. A natural application of this technique would be to slightly overdoped cuprates. For these materials, a model of a 2D metal with a small *d*-wave pseudogap (that is starting to emerge with reduced doping) is a plausible description of the metallic state at fields above H_{C2} and semiclassical calculations of ρ_{zz} may adequately capture transport properties. If the magnitude of the gap is small then it will not appreciably reduce the density of states (or be observable in angle averaged transport measurements[21]) but, as revealed below, can still have a significant effect on the field-angle dependence of the interlayer resistivity. To extract from ρ_{zz} information about the doping, temperature, and field dependence of $\Delta_{\mathbf{k}}$ would be of great value toward understanding the relationship between the pseudogap and superconductivity.[22,23] The effects of a nonzero $\Delta_{\mathbf{k}}$ may already be present in existing interlayer resistance data on slightly overdoped cuprates, convoluted with the effects of anisotropic scattering.[24] If so, a reinterpretation of these data using models that incorporate a pseudogap could be fruitful.

We study a model with well-defined electronic quasiparticles existing in the presence of a *d*-wave pseudogap in the density of states. The manner in which the opening of the pseudogap will change the interlayer resistivity is predicted and the following main results obtained: (i) an expression for the interlayer resistance ρ_{zz} in the semiclassical limit in a strong magnetic field of arbitrary strength and direction. (ii) For the simple case of a field parallel to the layer with arbitrary intralayer orientation ϕ_B, the quantitative effect of a pseudogap on $\rho_{zz}(\phi_B)$ is calculated using a realistic model band structure. The average magnitude of $\rho_{zz}(\phi_B)$ varies nonmonotonically with the size of the pseudogap while its ϕ_B dependence is modified in a manner distinctive of the pseudogap symmetry. A strongly anisotropic normal state $\rho_{zz}(\phi)$ is smoothed by the pseudogap through the introduction of new low-energy current contributions associated with *d*-wave nodes.

Considering our results in light of the success of the angle-dependent magnetoresistance oscillations (AMRO) technique in extracting band structure and scattering parameters of cuprates, we propose that this technique should also prove to be a viable means of obtaining a *T*-, *B*-, and doping-dependent parametrization of the *d*-wave pseudogap. The characterization of the pseudogap at high fields and low temperatures, following this approach, would be complementary to the array of other experimental probes of the anisotropic pseudogap and would likely provide unique insight. The anisotropic interlayer resistance technique is a bulk probe, can be carried out under high magnetic fields (thereby accessing

the low-temperature field-induced normal state) and enables a **k**-space mapping with good angular resolution.

II. SEMICLASSICAL PICTURE OF PSEUDOGAP STATE

As a simple model of the *d*-wave pseudogap state one can use the normal (diagonal) part of the BCS Green's function, taking the anomalous part equal to zero. The Green's function is

$$G_0(\omega,\mathbf{k},x) = \left(\frac{u_{\mathbf{k}}^2}{\omega - E_{\mathbf{k}}} + \frac{v_{\mathbf{k}}^2}{\omega + E_{\mathbf{k}}}\right) \tag{1}$$

with band energy $\xi_{\mathbf{k}}$, pseudogap $\Delta_{\mathbf{k}}$ and relative spectral weights for the electron and hole terms

$$u_{\mathbf{k}}^2 = \frac{1}{2}(1 + \xi_{\mathbf{k}}/E_{\mathbf{k}}), \quad v_{\mathbf{k}}^2 = \frac{1}{2}(1 - \xi_{\mathbf{k}}/E_{\mathbf{k}}) \tag{2}$$

and a quasiparticle energy $E_{\mathbf{k}}$ given by

$$E_{\mathbf{k}} = \sqrt{\xi_{\mathbf{k}}^2 + \Delta_{\mathbf{k}}^2}. \tag{3}$$

In Ref. 25, several model Green's functions for the pseudogap state are discussed with their associated spectral functions compared to photoemission spectroscopy (ARPES) data (in particular, with the observed Fermi arcs in far-underdoped samples). Equation (1), which is particle-hole symmetric, is discussed along with Green's functions that, while similar in structure to Eq. (1), include particle-hole symmetry-breaking terms or multiple scattering lifetimes. These alternative models include the YRZ ansatz, discussed in Refs. 26–28, and a commensurate spin-density-wave picture[29] [in which electrons on the Fermi surface at **k** are coupled via the pseudogap $\Delta_{\mathbf{k}}$ to those at $\mathbf{k}+\mathbf{Q}$ where $\mathbf{Q}=(\pi,\pi)$]. In all of these models the underlying Fermi surface, which is described by a tight-binding model and resembles the experimental Fermi surface of the overdoped systems, is modified by a nonzero *d*-wave pseudogap: turning on the pseudogap introduces low-energy elliptical contours near the $(\pi/2,\pi/2)$ points in the Brillouin zone (and gaps out excitations elsewhere on the overdoped Fermi surface). Each model enjoys partial success in accounting for the ARPES data (the experimental picture is still unfolding and it is too early to say which model will ultimately provide the most complete description) and can be viewed as a candidate model of the fermionic quasiparticles in cuprates. The interlayer resistance of any of these models could be studied using the approach followed in this paper. We consider here only the particle-hole symmetric expression [Eq. (1)] in order to illustrate, in the simplest context, the qualitative changes to the normal metal ρ_{zz} that are induced by turning on a small pseudogap $\Delta_{\mathbf{k}}$.

Equation (1) can be viewed as a description of a two-band metal with band energies of $\pm E_{\mathbf{k}}$, measured from the Fermi level, and **k**-dependent spectral weights. At $T=0$ the lower band is filled, the upper band empty and their nodal crossing point lies exactly at the chemical potential. If the imaginary part of the self-energy correction to Eq. (1) is small (compared to relevant ω) then the quasiparticles in each band are well defined and transport properties can be calculated using a semiclassical Boltzmann approach.

For the semiclassical picture to be applicable, the quasiparticles in each band must remain well defined, i.e., the imaginary parts of the self-energy correction to Eq. (1) must be small compared to relevant frequencies ω. At low temperature and frequency, impurity scattering will dominate. The associated scattering rate can be obtained following the procedure for *d*-wave superconductors[30] and it is known that at sufficiently low frequency the impurity scattering rate becomes larger than the frequency so the semiclassical picture of transport is not applicable. At high temperature and frequency, strong inelastic scattering will also render the semiclassical approach invalid. However there may exist an intermediate frequency range for which both the impurity and inelastic-scattering rates are relatively small. In this range, quasiparticles are sharply defined and the scattering rate $\tau^{-1}(\omega,\mathbf{k})$ can be evaluated at the quasiparticle pole $\omega=E_{\mathbf{k}}$. We assume that such a frequency range exists and calculate the interlayer resistivity in a magnetic field using Boltzmann theory.

III. INTERLAYER RESISTANCE IN THE PSEUDOGAP STATE IN THE PRESENCE OF AN ARBITRARY MAGNETIC FIELD

To have interlayer current there must be a finite amplitude $t_\perp$ for hopping between adjacent layers. However, according to Kennett and McKenzie,[13] the form of the interlayer conductivity does not depend on whether or not interlayer transport is coherent (i.e., it does not depend on the relative magnitude of $t_\perp$ and $\hbar\tau^{-1}$) as long as in-plane momentum is conserved during interlayer hopping. We may thus carry out the calculation of the interlayer conductivity by supposing that a three-dimensional Fermi (quasicylindrical) Fermi surface exists even when we are in the regime in which the Bloch vector in the interlayer direction k_z is not well defined. Taking advantage of this, we simply add to $E_{\mathbf{k}}$ a term $-2t_\perp(k_x,k_y)\cos(k_z c)$ where $t_\perp(k_x,k_y)$ is the interlayer hopping coefficient and c the distance between layers. The associated interlayer velocity is $v_z(k_x,k_y,k_z)=2c\hbar^{-1}t_\perp(k_x,k_y)\sin(k_z c)$. The calculation of the interlayer current is done to lowest order in v_z.

The Boltzmann equation in a weak electric field Ξ along the z axis and a magnetic field **B** of arbitrary strength and direction is

$$\frac{\partial g_{\mathbf{k}}}{\partial t} - I[g_{\mathbf{k}}] = -e\Xi v_z(\mathbf{k})\left(-\frac{df_0}{dE_{\mathbf{k}}}\right), \tag{4}$$

where the total distribution is $f=f_0+f_1$ with $f_1=-(df_0/dE_{\mathbf{k}})g$, $f_0(x)$ is the Fermi function, and $I[g]$ is the collision functional. The auxiliary time variable t is defined by the equation of motion[31]

$$\frac{d\mathbf{k}}{dt} = -e\mathbf{v}_g \times \mathbf{B}, \tag{5}$$

where $\mathbf{v}_g = dE_{\mathbf{k}}/d\mathbf{k}$. Equations (5) and (4) are solved to obtain the distribution function, which is inserted into the expression for the interlayer current

$$j_z(t) = \frac{2e}{2\pi^3}\int d\mathbf{k} v_z(\mathbf{k}[t]) f_1(t,\mathbf{k}[t]). \tag{6}$$

The current is found by taking a t-Fourier transform of $j_z(t)$ and evaluating in the zero-frequency limit. The spectral weights from the two bands combine simply to give $u_{\mathbf{k}}^2+v_{\mathbf{k}}^2=1$ for the particle-hole symmetric case.

For a field $\mathbf{B}=B(\sin\theta_B\cos\phi_B,\sin\theta_B\sin\phi,\cos\theta_B)$, Eq. (5) gives $d\phi/dt=\omega_C(E,\phi,\theta_B)$ where the cyclotron frequency is

$$\hbar\omega_C(E,\phi,\theta_B)=eB\cos\theta_B\frac{\mathbf{v}_g\cdot\mathbf{k}_E}{k_E^2}. \tag{7}$$

The cylindrical ϕ variable parameterizes the cyclotron orbit around a closed energy contour $E_{\mathbf{k}}=E$. Any point $\mathbf{k}_E$ on the projection of this contour onto the k_x-k_y plane is written as $\mathbf{k}_E=k_E(\phi)(\cos\phi,\sin\phi)$ where $k_E(\phi)$ is the radial cylindrical distance measured from some arbitrary point in the region enclosed by the contour. In the normal state we can use a single energy contour (the Fermi surface) $\mathbf{k}_E=\mathbf{k}_f=k_f(\phi)(\cos\phi,\sin\phi)$.

The k_z momentum varies according to

$$\frac{dk_z}{dt}=-\tan\theta_B\frac{d}{dt}[k_E(\phi)\cos(\phi-\phi_B)], \tag{8}$$

which results in a periodic oscillation of the interlayer velocity $v_z(k_z[t])$ that is determined by the direction of the field angle θ_B.

Finally, since $E_{\mathbf{k}}$ is independent of k_z in the collision functional, the integral over k_z of the "scattering-in" term vanishes by symmetry (this is true not only for scattering from point defects but for any other scattering mechanism that can be regarded as spatially confined to a single plane[15,18]). We are left with a relaxation-time description: $I[g_{\mathbf{k}}]=-g_{\mathbf{k}}/\tau(E_{\mathbf{k}})$ with the current relaxation rate equal to the total quasiparticle scattering rate $\tau^{-1}(\omega=E_{\mathbf{k}})$. The fact that vertex corrections vanish to lowest order in v_z in the calculation of the interlayer resistivity is a considerable simplification. It means that we can use any appropriate model for the scattering rate, including elastic or inelastic scattering or even a sum over several different mechanisms.

We insert these expressions into Eq. (4), formally solve for $g_{\mathbf{k}}(t)$ and use this in Eq. (6) to obtain the interlayer conductivity $\sigma_{zz}=1/\rho_{zz}$

$$\sigma_{zz}(\mathbf{B})=A\int_{-\infty}^{+\infty}\frac{dE(-df_0/dE)}{1-P(E)}, \tag{9}$$

$$\times\int_0^{2\pi}\frac{d\phi_2 t_\perp(\phi_2)}{\hbar\omega_C(\phi_2)}\int_{\phi_2-2\pi}^{\phi_2}\frac{d\phi_1 t_\perp(\phi_1)}{\hbar\omega_C(\phi_1)}M(\phi_1,\phi_2), \tag{10}$$

where

$$A=\frac{e^2}{\hbar\pi^2}ceB\cos\theta_B,$$

$$M(\phi_1,\phi_2)=G(\phi_1,\phi_2)\cos\Phi[\phi_1,\phi_2],$$

$$G(\phi_1,\phi_2)=\exp\left[-\int_{\phi_1}^{\phi_2}\frac{d\phi'}{\omega_C(\phi')\tau(\phi)}\right],$$

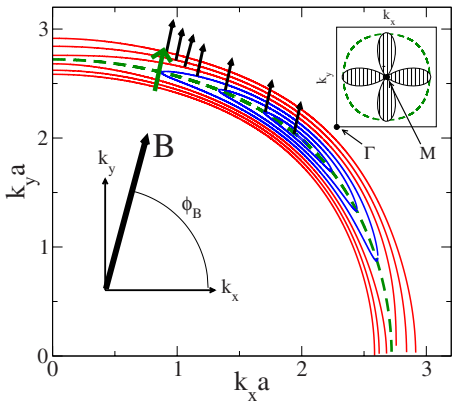

FIG. 1. (Color online) A small pseudogap reduces the dependence of ρ_{zz} on the direction ϕ_B of a magnetic field $\mathbf{B}$ parallel to the layers. Upper inset: the dashed (green) curve is a Fermi surface, closed around the corner M point of the square Brillouin zone, and the hatched curve indicates the magnitude of the d-wave pseudogap. Main panel: when the field is large, the interlayer current is dominated by $\mathbf{k}$ points on low-lying energy $E_{\mathbf{k}}$ contours at which the electron velocity $\mathbf{v}_g=dE_{\mathbf{k}}/d\mathbf{k}$ is parallel to $\mathbf{B}$. The solid curves show low-lying $E_{\mathbf{k}}$ contours (moving outward from the node, the contours are for $E/\Delta_0=0.05,0.5,1,1.5,2,2.5,3$) in the upper right quadrant of the $\mathbf{M}$-centered Brillouin zone. The arrows (each parallel to $\mathbf{B}$) are located at the dominant $\mathbf{k}$ point for each contour. In the normal state, the dominant $\mathbf{k}$ is the point where the largest (green) arrow intersects the dashed (Green) Fermi surface. In the pseudogap state, the dominant $\mathbf{k}$ are spread over a large range that extends from the normal-state point (for $E_{\mathbf{k}}>\max\Delta_{\mathbf{k}}$) to the node (for $E_{\mathbf{k}}\ll\max\Delta_{\mathbf{k}}$). The opening of a pseudogap effectively spreads the current contribution over the Fermi surface, thereby smearing the ϕ_B dependence of ρ_{zz}.

$$\frac{\Phi(\phi_1,\phi_2)}{c\tan\theta_B}=\left[k_E(\phi_1)\cos(\phi_1-\phi_B)-k_E(\phi_2)\cos(\phi_2-\phi_B)\right]$$

and $P=G(0,2\pi)$. The function $G(\phi_1,\phi_2)$ is the probability that a quasiparticle can proceed from ϕ_1 to ϕ_2 along its cyclotron orbit without being scattered so P is the probability that a quasiparticle completes an orbit.

Equation (9) has been written in the same form as the corresponding expression for a normal metal.[13] However $\omega_C(\phi)$, τ, $k_E(\phi)$, and P all *depend on energy* in the pseudogap state (though we have not always written this explicitly). Moreover, the ϕ and $k_E(\phi)$ variables must be interpreted differently in this expression depending on whether the energy is greater or less than $\max\Delta_{\mathbf{k}}$. This is because these variables are defined with reference to a closed 2D cyclotron orbit but the orbits (i.e., the energy contours) have different topologies depending on the relative size of E and $\max\Delta_{\mathbf{k}}$ as shown in Fig. 1. For $E<\max\Delta_{\mathbf{k}}$ there are four equivalent (banana-shaped) contours closed around nodal points so a node can be taken as an orbit center with the polar-angle ϕ parameterizing position along the contour. Thus $k_E(\phi)$, which is measured from the node to the contour, depends strongly on both E and ϕ. (We should include an overall sum over the four nodes in Eq. (9), though this has not been written explicitly. There is no mixing of different nodes since an electron remains on a single nodal contour

during cyclotron motion and the current contribution from each nodal region can be obtained separately. For $E > \max \Delta_{\mathbf{k}}$ a single contour encircles the entire normal-state Fermi surface and $k_E(\phi)$, measured from a central point, is weakly anisotropic, i.e., its anisotropy is that of the normal-state Fermi surface. The energy integral in Eq. (9) must be broken up into low- and high-energy regions with the $k_E(\phi)$ variable defined accordingly.

Equation (9) is the main result of this paper. This expression could be used in fitting procedures similar to those applied in the normal state of overdoped cuprates. The magnitude of the pseudogap as, say, a function of doping, temperature, and field strength in overdoped systems could then be extracted. A typical set of fitting parameters might include hopping amplitudes describing the normal-state band structure and interplane hopping magnitude $t_\perp$ (the values of which would be constrained by independent measurements and would be expected to be independent of temperature and weakly dependent on doping), the normal-state scattering rate τ^{-1} (which can also be independently estimated) and the gap magnitude. Additional parameters could be incorporated if one were to go beyond the nearest-neighbor expression for $\Delta_{\mathbf{k}}$ or to include anisotropy in the scattering rate. Overall, the number of parameters would not have to exceed that used in previous normal-state analysis.

We will not undertake detailed numerical evaluations of Eq. (9) in this paper but will discuss, in the remainder of this section, some of the general features of this expression that distinguish it from the familiar normal-state result. The contribution to the conductivity, Eq. (9), that comes from energies $E \gg \max \Delta_{\mathbf{k}}$ will be identical to the normal-state expression. So, the total conductivity is a weighted sum of the normal-state value and the low-energy (i.e., $E_{\mathbf{k}} < \max \Delta_{\mathbf{k}}$) contribution associated with the pseudogap. The relative weighting is controlled by the value of Δ_0/k_BT. The properties of the low-energy (pseudogap) contribution to the conductivity are qualitatively different than those of the high-energy (normal-state) contribution. It is more strongly temperature dependent and is less sensitive to the direction of the magnetic field.

To get some feel for the low-energy contribution to the magnetoconductivity, associated with the pseudogap, we consider the nodal limit $E \ll \Delta_0$ for which $\Delta_{\mathbf{k}}$ and $\xi_{\mathbf{k}}$ can be linearly expanded about nodal points. In the nodal limit we write $\Delta_{\mathbf{k}} = v_2 k_2$ and $\xi_{\mathbf{k}} = v_f k_1$ where k_2 and k_1 are momenta parallel and perpendicular to the Fermi surface, respectively. The radius of the energy contour with energy E is given by

$$\hbar k_E(E,\phi) = \frac{E}{\sqrt{v_f^2 \cos^2(\phi - \phi_n) + v_2^2 \sin^2(\phi - \phi_n)}} \tag{11}$$

and the cyclotron frequency is

$$\omega_C(\phi,E) = eB \cos\theta_B E^{-1}[v_f^2 \cos^2(\phi - \phi_n) + v_2^2 \sin^2(\phi - \phi_n)], \tag{12}$$

where ϕ_n is the direction of the node ($\phi_n = \pm\pi/4, \pm 3\pi/4$). Since $v_f \gg v_2$ the energy contour is a narrow ellipse and the cyclotron motion of the quasiparticle slows down dramatically as it crosses the Fermi surface $k_1 = 0$.

If the probability P is small, then quasiparticles are unlikely to complete cyclotron orbits without being scattered and the field dependence of the conductivity is weak. The field-dependent effects of interest (i.e., the sensitivity of σ_{zz} to in-layer anisotropy and the AMRO) occur when P is of order 1. The quantity P depends on the scattering mechanism and, generally in the pseudogap state, on energy E. In the simple case of point defects, the scattering rate[30] is approximately given by

$$\tau^{-1}(E) = \tau_0^{-1}[\nu(E)/\nu_0]^\eta, \tag{13}$$

where τ_0^{-1} is the normal-state scattering rate, $\nu(E)$ and ν_0 are the densities of states in the pseudogap and normal states, respectively, and $\eta = +1$ (or -1) in the Born (or unitary) limit. For unitary scattering (to which we henceforth restrict ourselves) there is a cancellation in factors of the quasiparticle density of states so that P becomes energy independent. In this case, P has roughly the same value as in the normal state. So, in strong fields, we can ignore the effects of scattering [i.e., set $G(\phi_1, \phi_2) = 1$] in both the high-energy (normal-state) contribution and the low-energy (nodal limit) contribution to σ_{zz}. This simplifies the following discussion.

Both the sensitivity of σ_{zz} to the anisotropy of the 2D band structure and the AMRO effect originate from the argument $\Phi(\phi_1, \phi_2)$ of the cosine in Eq. (9). The cosine oscillates rapidly when $k_f c \tan\theta_B$ is large and kills the integral everywhere except at special momentum directions, which depend on field orientation ϕ_B. As discussed in Ref. 13, the conductivity is thus dominated by the small region where both ϕ_1 and ϕ_2 are close to a special direction defined by the solution of

$$\frac{d}{d\phi}[k_f(\phi)\cos(\phi - \phi_B)] = 0. \tag{14}$$

Since the field direction ϕ_B determines the value of ϕ_1 and ϕ_2 that dominate the integrals, the band-structure parameters are evaluated at a symmetry-unique point on the Fermi surface that can be tuned by field direction, allowing the Fermi surface to be mapped out. Also, since the scale of the rapid oscillation is set by $k_f c \tan\theta_B$, the overall magnitude of the conductivity oscillates in θ_B with a period determined by this quantity (this is AMRO).

However, when we apply this reasoning to the low-energy pseudogap contribution, we find that such strong dependence on field-direction angle is not expected. The solution to Eq. (14) in the nodal limit is $\phi - \phi_n = \arctan[\alpha^2(\phi_B - \phi_n)]$ where $\alpha = v_f/v_2 \gg 1$. The large factor α^2 means that the dominant value of $\phi - \phi_n$ will almost always be close to $\pi/2$, i.e., close to the point at which the nodal energy contour crosses the Fermi surface, *independent* of the direction of field. (The only exception would be if the magnetic field were pointed precisely in a nodal direction.) So, the dependence on the field direction ϕ_B is far weaker in the low-energy pseudogap contribution than it is in the normal state. Moreover, the scale for the oscillatory dependence in the nodal limit is $k_E c \tan\theta_B \approx (E/v_2)c \tan\theta$. For energies $E \ll \Delta_0$ this quantity will be much smaller than one for any $\theta_B \neq \pi/2$. The argument of the cosine in Eq. (9) will be small and no oscillatory

dependence on field angle θ_B will be seen. Even at temperatures as high as $k_BT/\Delta_0 \approx 1$ we do not expect to see prominent AMRO coming from the pseudogap contribution to the conductivity. This is because the integral over energy will average k_E over all values from 0 to nearly k_f, giving no sharp period for oscillatory behavior.

These qualitative arguments suggest that the low-energy (pseudogap) contribution to the conductivity will not show the strong field-direction dependence characteristic of the high-energy (normal-state) contribution. (A detailed analysis is needed, however, to account for the strong energy dependence of the scattering rate that could change this picture by giving dominant weight in the integral to a particular energy range.) So, the onset of the pseudogap should have the generic effect of smoothing the dependence on field angle. Nevertheless, this smoothing will proceed in a particular manner that is *characteristic of the anisotropy of the pseudogap*. None of the above effects would occur for an isotropic pseudogap and the *d*-wave case discussed here could be distinguished from alternative forms since the arrangement of nodal points would have a different relationship with the normal-state band anisotropy.

In the next section we consider the simple limit of a field in the layers, i.e., $\theta_B = \pi/2$. This is done to provide a more quantitative description of the effect that a pseudogap has on the field-direction anisotropy of $\rho_{zz}(\phi_B)$. Also, theoretical expressions for ρ_{zz}, with which we can compare our results, have been obtained previously using a different formalism.

IV. CASE OF A FIELD PARALLEL TO THE LAYERS

The general result Eq. (9) can be evaluated in the limit $\theta_B \rightarrow \pi/2$ (i.e., for the case of a field in the layers) by employing a stationary phase approximation but it is simpler to go back to the beginning of the derivation and make this assumption. When **B** is in the layers

$$\sigma_{zz} = \frac{e^2 c}{\hbar \pi^2} \int d^2\mathbf{k} \left(-\frac{df_0}{dE_\mathbf{k}} \right) t_\perp^2(\mathbf{k}) \frac{\tau^{-1}(E_\mathbf{k})}{\tau^{-2}(E_\mathbf{k}) + \Omega_C(\mathbf{k})^2}, \quad (15)$$

where **k** is the momentum in the plane and

$$\Omega_C(\mathbf{k}) = ec|\mathbf{v}_g \times \mathbf{B}|. \quad (16)$$

In the normal state, $\tau^{-1}(E) = \tau^{-1}$ and $\Omega_C(\mathbf{k}) = \Omega_C(\phi)$ are both independent of energy so the integral over $E_\mathbf{k}$ gives unity and Eq. (15) reduces to a Fermi-surface average. The magnetic field becomes important when the ϕ-averaged quantity $\Omega_C \approx ecv_fB$ becomes comparable to the scattering rate $1/\tau$. Note that the criterion for field effects $\Omega_C\tau \gtrapprox 1$ is more favorable by a factor of k_fc than the corresponding criterion for in-layer transport, where $k_fc \approx 10$ is typical in cuprates.[4]

Equation (15) can also be obtained using a tunneling Hamiltonian approach and a similar result was thus obtained in Ref. 34. The tunneling current is expressed as a convolution of spectral functions on adjacent layers. The gauge can be chosen such that the difference in the vector potential between adjacent layers is $\mathbf{A} = c(B_y, -B_x, 0)$ and the corresponding spectral functions differ only by a momentum shift equal to $e\mathbf{A}$. Evaluating the spectral functions in the quasiparticle approximation and using $\Omega_C \approx (E_{\mathbf{k}-e\mathbf{A}} - E_\mathbf{k})$ one obtains Eq. (15). The advantage of the semiclassical approach followed here is that it can be generalized to describe fields out of the layers [Eq. (9)]. In the remainder of this paper we will, however, focus on the simple case of Eq. (15). We go beyond the $k_BT \ll \Delta_0$ nodal limit considered in Ref. 34 to consider arbitrary k_BT/Δ_0 and a realistic normal-state band structure for cuprates in order to study the effect of a small pseudogap on the ϕ_B dependence of ρ_{zz}.

In a strong magnetic field, $\Omega_C\tau \gg 1$ so $\Omega_C(\phi_B)\tau \gg 1$ at typical ϕ_B, the Fermi-surface average in Eq. (15) is dominated by the **k** values for which $\Omega_C(\mathbf{k}) = 0$, i.e., by **k** for which the quasiparticle velocity is parallel to **B**. This means that the normal-state interlayer resistivity is determined by the values of band parameters at a particular point on the Fermi surface $\mathbf{k} = \mathbf{k}^* = k_f(\phi^*)(\cos\phi^*, \sin\phi^*)$ where the value of ϕ^* is controlled by ϕ_B (in an isotropic system $\phi_B = \phi^*$). Moreover, the resistivity is independent of τ^{-1} in strong fields since the current is limited by classical magnetoresistance rather than scattering. Upon varying ϕ_B, one can use ρ_{zz} to effectively map out the ϕ dependence of the in-plane band parameters.

In the pseudogap state, the energy dependence of $\Omega_C(\mathbf{k})$ changes this simple picture as illustrated in Fig. 1. For energies $E_\mathbf{k} \gg \max \Delta_\mathbf{k}$, the energy contours of the pseudogap state are almost identical to the Fermi surface itself. So the contribution to ρ_{zz} that comes from energies much larger than $\max \Delta_\mathbf{k}$ are the same as in the normal state. However, when a pseudogap opens up (i.e., once Δ_0 becomes comparable to k_BT) the conductivity begins to receive significant contributions from energies $E_\mathbf{k} < \max \Delta_\mathbf{k}$. The associated low-energy energy contours are centered on nodes and the **k** point on such an energy contour where $\Omega_C(\mathbf{k})$ vanishes is far removed from the corresponding normal-state point $\mathbf{k}^*$. This means that a small pseudogap results in contributions to ρ_{zz} coming from a much broader range on the Fermi surface, thereby weakening the ϕ_B dependence.

This loss of ϕ_B dependence occurs initially without a corresponding increase in the magnitude of σ_{zz}. In fact, the effect of turning on a small pseudogap in the presence of a strong in-layer magnetic field is to *decrease* the ϕ_B averaged interlayer resistivity as shown in Fig. 2. This comes about because classical magnetoresistance is relieved by the pseudogap, both through a reduction in the average quasiparticle velocity and through the increased range of **k** that contribute to the current. The effect is independent of τ^{-1} at large fields, as noted above, so the energy dependence of the scattering rate (i.e., whether we are in the Born or unitary limit) does not matter. For a sufficiently large pseudogap, the reduction in the carrier density overcomes this effect, so ρ_{zz} reaches a minimum at $\Delta_0/k_BT \approx 1$ and thereafter increases, eventually becoming very large for $\Delta_0/k_BT \gg 1$ when the current comes only from the nodal regions.

V. CALCULATION OF INTERLAYER RESISTIVITY USING MODEL BAND STRUCTURE OF Tℓ2201

To obtain a more quantitative picture of the ϕ_B dependence of ρ_{zz} we use band-structure parameters obtained from

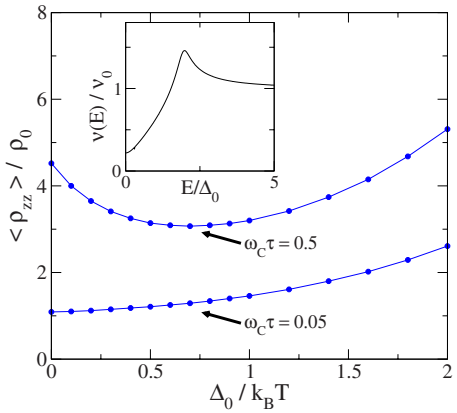

FIG. 2. (Color online) The nonmonotonic dependence of the interlayer resistivity ρ_{zz} on the magnitude of a d-wave pseudogap. Main panel: the vertical axis is the interlayer resistivity, averaged over the direction of the in-layer magnetic field ϕ_B, in units of the normal-state zero-field value ρ_0. The horizontal axis is the magnitude of the d-wave pseudogap and the different curves are for different field strengths. For weak fields ($\omega_C\tau \ll 1$), turning on the gap has no effect other than reducing the carrier density so the resistance increases with Δ_0/k_BT. In strong fields, the opening of a small gap reduces the average quasiparticle velocity and the associated Lorentz force responsible for the large magnetoresistance. This effect results in an initial drop in the interlayer resistance. As Δ_0/k_BT becomes large, the reduction in carrier density eventually overrides this effect and ρ_{zz} begins to increase. Upper inset: the pseudogap density of states $\nu(E)$ in terms of the normal-state value ν_0. The scattering rate τ^{-1} depends on E through the density of states.

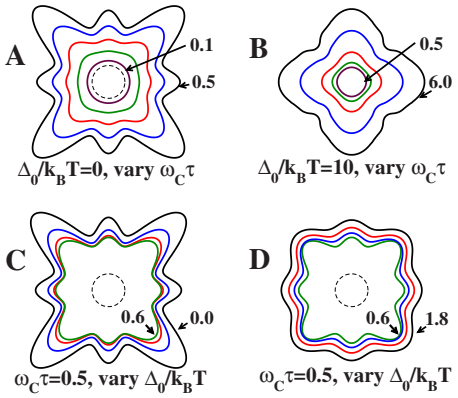

FIG. 3. (Color online) Anisotropy of the interlayer resistance ρ_{zz} in the normal and d-wave pseudogap states. Solid curves are polar plots of ρ_{zz}/ρ_0 versus ϕ_B where a crystal axis is along the horizontal and the band structure of Tℓ2201 has been used. The dashed curve is the unit circle (unseen in panel B, where the radial scale is much larger). Panel A: the normal state (constant $\Delta_0/k_BT=0$) for varying field strength; the solid curves from inside out are for: $\omega_C\tau = 0.1, 0.2, 0.3, 0.4, 0.5$. Panel B: the low-temperature pseudogap state ($\Delta_0/k_BT=10$) for varying field strength; the solid curves from inside out are for: $\omega_C\tau=0.5, 1, 2, 4, 6$. Panels C and D: a large applied field (constant $\omega_C\tau=0.5$) with varying pseudogap magnitude. The solid curves in C are, from outside in: $\Delta_0/k_BT=0, 0.2, 0.4, 0.6$ and in D, from inside out: $\Delta_0/k_BT=0.6, 1.0, 1.4, 1.8$. The resistance first decreases (in C) then increases (in D) as the pseudogap grows. The angle dependence is reduced by the opening of a pseudogap and is eventually replaced by that associated with the anisotropic gap itself.

ARPES and interlayer resistance data on the two-layer cuprate Tℓ2201. The ARPES data[32] can be reasonably fit by a tight-binding model with nearest and next-nearest hopping parameters: $\xi_{\mathbf{k}} = -2t[\cos k_x + \cos k_y] - 4t' \cos k_x \cos k_y - \xi_0$ with $\mathbf{k}$ measured from $(\pi/a, \pi/a)$, $t'/t = 0.42$ and $\xi_0/t = 1.36$. The resulting Fermi surface is shown in Fig. 1. In this material the interlayer hopping parameter $t_\perp(k_x, k_y)$ vanishes by symmetry at eight points on the Fermi surface (along $k_x = k_y$ and $k_x = 0$ directions). It can be modeled (according to AMRO data[1]) as $t_\perp(\phi) = t_\perp[\sin 2\phi + k_6 \sin 6\phi + (k_6 - 1.0)\sin 10\phi]$ with $k_{10} = k_6 - 1.0$ and $k_6 = 0.71$. The energy scale $t_\perp$ can be absorbed into the zero-field, normal-state resistivity but the large anisotropy in $t_\perp(\phi)$ contributes to the strong ϕ_B dependence observed for this material in the normal state. Moreover, since $t_\perp(\phi)$ vanishes at the nodes, the magnitude of ρ_{zz} becomes extremely large in the nodal limit $\Delta_0/k_BT \gg 1$.

The anisotropic magnetoresistance in the normal state is illustrated[33] in the polar plots of $\rho_{zz}(\phi_B)/\rho_0$ versus ϕ_B in panel A of Fig. 3. A field of $\omega_C\tau \approx 0.5$ is sufficient to reveal the strong anisotropy of the underlying band structure. (For the low-temperature scattering rate reported[2] for Tℓ2201, this value of $\omega_C\tau$ is achieved for fields of approximately 50 T.) Note also that the ϕ_B-averaged magnitude of ρ_{zz}/ρ_0 decreases as the scattering rate increases for a given field strength. In panel B, the nodal limit $\Delta_0/k_BT \gg 1$ of ρ_{zz}/ρ_0 is depicted. Here the current is coming entirely from momenta near the nodes and thus *provides no information about the normal-state band parameters elsewhere on the Fermi surface*. The anisotropy, which has been discussed in Ref. 34, results from unequal, and ϕ_B-dependent, contributions from different nodes owing to the large ratio of v_f/v_2 where v_f is the Fermi velocity is the "gap" velocity.

Panels C and D of Fig. 3 describe the effect that turning on a d-wave pseudogap has on $\rho_{zz}(\phi_B)$ in a relatively strong field ($\omega_C\tau = 0.5$). The scattering rate was evaluated in the unitary limit, using the rounded density of states plotted in Fig. 2. In panel C, which shows small values of Δ_0/k_BT, the magnitude of ρ_{zz} decreases as the gap opens. In panel D, which shows larger values of Δ_0/k_BT, the ϕ_B-averaged resistance has already reached its minimum value, depicted in Fig. 2 and is thus growing with Δ_0/k_BT.

It is seen, by comparing panels A and C that the initial effect of a small gap on $\rho_{zz}(\phi_B)$ is similar to the effect of an enhancement in the scattering rate. The reason for this similarity follows from the discussion of Fig. 1: the pseudogap increases the band of $\mathbf{k}$ points that contribute to the interlayer current just as would an increase in τ^{-1}. The manner by which the ϕ_B dependence changes as the pseudogap continues to grow in magnitude is, however, very different from that resulting from an increase in the scattering rate. Not only does the magnitude of ρ_{zz} vary nonmonotonically with Δ_0/k_BT but also $\rho_{zz}(\phi_B)$ evolves to incorporate the anisotropy of $\Delta_{\mathbf{k}}$ along with that already coming from $t_\perp(\phi)$ and the intralayer band parameters. Given the success of the angle-dependent interlayer resistance technique in extracting precise values for several band-structure parameters, it appears that this technique should be equally capable of obtain-

ing both the magnitude and anisotropy of a pseudogap as it emerges in the over or near optimally doped cuprates.

VI. CONCLUSIONS

Measurements of the interlayer resistivity in layered metals, made in a magnetic field with varying orientation, can be used to characterize anisotropic properties within individual layers. Among these properties, band-structure parameters and the inelastic-scattering rate in various systems have already been extracted by this method. In this paper we have extended the analysis of such measurements to incorporate a pseudogap with *d*-wave symmetry. A general expression for the interlayer resistivity in the pseudogap state was obtained via a semiclassical calculation.

For a field along the layers, the main effect of a small pseudogap is to smooth the dependence of the resistivity on the in-layer field direction ϕ_B. This occurs because while electrons only contribute to the normal-state interlayer current if they are located at a particular point on the Fermi surface so that they have a velocity parallel to the magnetic field, quasiparticles with an energy smaller than the pseudogap can contribute to the interlayer current from anywhere on the Fermi surface. The average magnitude of the interlayer resistivity first decreases then subsequently increases as the pseudogap opens, reaching a minimum value when the magnitude of the pseudogap is comparable to the temperature. We hope that this work will stimulate new experiments and analysis to detect the presence and map the anisotropy of a pseudogap in layered strongly correlated materials.

ACKNOWLEDGMENTS

We thank Matthew French and Nigel Hussey for helpful discussions and for sharing with us unpublished data. This work has been supported by the Australian Research Council.

*mfsmith@physics.uq.edu.au

[1] N. E. Hussey, M. Abdel-Jawad, A. Carrington, A. P. Mackenzie, and L. Balicas, Nature (London) **425**, 814 (2003).
[2] M. Abdel-Jawad, M. P. Kennett, L. Balicas, A. Carrington, A. P. Mackenzie, R. H. McKenzie, and N. E. Hussey, Nat. Phys. **2**, 821 (2006).
[3] M. Abdel-Jawad, J. G. Analytis, L. Balicas, A. Carrington, J. P. H. Charmant, M. M. J. French, and N. E. Hussey, Phys. Rev. Lett. **99**, 107002 (2007).
[4] J. G. Analytis, M. Abdel-Jawad, L. Balicas, M. M. J. French, and N. E. Hussey, Phys. Rev. B **76**, 104523 (2007).
[5] C. Bergemann, A. P. Mackenzie, S. R. Julian, D. Forsythe, and E. Ohmichi, Adv. Phys. **52**, 639 (2003).
[6] L. Balicas, S. Nakatsuji, D. Hall, T. Ohnishi, Z. Fisk, Y. Maeno, and D. J. Singh, Phys. Rev. Lett. **95**, 196407 (2005).
[7] M. V. Kartsovnik, Chem. Rev. **104**, 5737 (2004).
[8] J. Wosnitza, *Fermi Surfaces of Low Dimensional Organic Metals and Superconductors* (Springer-Verlag, Berlin, 1996).
[9] T. Osada, H. Nose, and M. Kuraguchi, Physica B: Condensed Matter **294-295**, 402 (2001).
[10] U. Beierlein, C. Schlenker, J. Dumas, and M. Greenblatt, Phys. Rev. B **67**, 235110 (2003).
[11] K. Enomoto, S. Uji, T. Yamaguchi, T. Terashima, T. Konoike, M. Nishimura, T. Enoki, M. Suzuki, and I. S. Suzuki, Phys. Rev. B **73**, 045115 (2006).
[12] K. G. Sandeman and A. J. Schofield, Phys. Rev. B **63**, 094510 (2001).
[13] M. P. Kennett and R. H. McKenzie, Phys. Rev. B **76**, 054515 (2007).
[14] M. P. Kennett and R. H. McKenzie, Physica B: Condensed Matter **403**, 1552 (2008).
[15] B. W. Brinkman and M. P. Kennett, Phys. Rev. B **80**, 094505 (2009).
[16] N. E. Hussey, M. Abdel-Jawad, L. Balicas, M. P. Kennett, and R. H. McKenzie, Physica B **403**, 982 (2008).
[17] J. Singleton, P. A. Goddard, A. Ardavan, A. I. Coldea, S. J. Blundell, R. D. McDonald, S. Tozer, and J. A. Schlueter, Phys. Rev. Lett. **99**, 027004 (2007).
[18] M. F. Smith and R. H. McKenzie, Phys. Rev. B **77**, 235123 (2008).
[19] L. Taillefer, Nat. Phys. **2**, 809 (2006).
[20] M. M. J. French, J. G. Analytis, A. Carrington, L. Balicas and N. E. Hussey, arXiv:0905.2504, New J. Phys. (to be published).
[21] W. Yu, B. Liang, and R. L. Greene, Phys. Rev. B **74**, 212504 (2006).
[22] M. R. Norman, D. Pines, and C. Kallin, Adv. Phys. **54**, 715 (2005); P. A. Lee, N. Nagaosa, and X.-G. Wen, Rev. Mod. Phys. **78**, 17 (2006).
[23] S. Hufner, M. A. Hossain, A. Damascelli, and G. A. Sawatzky, Rep. Prog. Phys. **71**, 062501 (2008).
[24] N. E. Hussey, private communication.
[25] M. R. Norman, A. Kanigel, M. Randeria, U. Chatterjee, and J. C. Campuzano, Phys. Rev. B **76**, 174501 (2007).
[26] K.-Y. Yang, T. M. Rice, and F.-C. Zhang, Phys. Rev. B **73**, 174501 (2006).
[27] K.-Y. Yang, H.-B. Yang, P. D. Johnson, T. M. Rice, and F.-C. Zhang, EPL **86**, 37002 (2009).
[28] K. Le Hur and T. M. Rice, Ann. Phys. **324**, 1452 (2009).
[29] S. Chakravarty, R. B. Laughlin, D. K. Morr, and C. Nayak, Phys. Rev. B **63**, 094503 (2001).
[30] H. Alloul, J. Bobroff, M. Gabay, and P. J. Hirschfeld, Rev. Mod. Phys. **81**, 45 (2009).
[31] We here use a classical force law in which the quasiparticle group velocity $\mathbf{v}_g = d E_{\mathbf{k}}/d\mathbf{k}$ couples to $\mathbf{B}$, which also follows from a straightforward replacement $\mathbf{k} \rightarrow \mathbf{k} - e\mathbf{A}$ in the spectral function appearing in the tunneling current. An alternative coupling [used in Ref. 34, see also Ref. 35)], is obtained by making the replacement as follows: $E_{\mathbf{k}-e\mathbf{A}} \rightarrow \sqrt{\xi^2_{\mathbf{k}-e\mathbf{A}} + \Delta^2_{\mathbf{k}}}$ so that the Lorentz force term is $e\mathbf{v}_b \times \mathbf{B}$ with $\mathbf{v}_b = (\xi_{\mathbf{k}}/E_{\mathbf{k}}) d\xi_{\mathbf{k}}/d\mathbf{k}$. As long as the magnitude of the pseudogap is small compared to the Fermi energy, the choice of $\mathbf{v}_g$ versus $\mathbf{v}_b$ makes little difference to interlayer current calculation with $\theta_B = \pi/2$.

[32] M. Platé, J. D. F. Mottershead, I. S. Elfimov, D. C. Peets, R. Liang, D. A. Bonn, W. N. Hardy, S. Chiuzbaian, M. Falub, M. Shi, L. Patthey, and A. Damascelli, Phys. Rev. Lett. **95**, 077001 (2005); D. C. Peets, J. P. F. Mottershead, B. Wu, I. S. Elfimov, R. Liang, W. N. Hardy, D. A. Bonn, M. Raudsepp, N. J. C. Ingle, and A. Damascelli, New J. Phys. **9**, 28 (2007).

[33] In constructing the plots of Fig. 3, we have not taken into account any potential field dependence of the magnitude of the pseudogap. One can interpret Δ_0 as the value of the pseudogap in the presence of a certain field B, the magnitude of which is parameterized by $\omega_C\tau$, and in this way allow for some B dependence of Δ_0 within these plots. In Ref. 36, an applied field of 60 T results in a reduction in the pseudogap (defined via T-dependent interlayer resistivity data) in slightly overdoped BSCCO by less than 30% from its zero-field value. On the other hand, fields of 50 T are sufficient, according to Ref. 2, to achieve values of $\omega_C\tau \approx 0.5$ in clean Tℓ2201 samples. It would thus appear that the field dependence of $\omega_C\tau$, and not that of Δ_0, would be most important in controlling the behavior of the interlayer resistivity over the parameter ranges considered in Fig. 3. So, while a field-dependent Δ_0 could be included for quantitative analysis, it is not expected to alter the qualitative picture described above.

[34] L. N. Bulaevskii, M. J. Graf, and M. P. Maley, Phys. Rev. Lett. **83**, 388 (1999).

[35] A. G. Aronov, Adv. Phys. **30**, 539 (1981).

[36] T. Shibauchi, L. Krusin-Elbaum, M. Li, M. P. Maley, and P. H. Kes, Phys. Rev. Lett. **86**, 5763 (2001).